

红色荧光粉 $\text{CePO}_4\text{-6LaPO}_4\text{@4SiO}_2\text{:Eu}^{3+}$ 的发光特性

刘 茹 王喜贵*

(内蒙古师范大学化学与环境科学学院, 呼和浩特 010022)

摘要: 采用溶胶凝胶-高温固相法制备 $\text{CePO}_4\text{-6LaPO}_4\text{@4SiO}_2\text{:Eu}^{3+}$ 荧光粉, 通过 XRD、TEM、EDS、IR 以及激发光谱和发射光谱对荧光粉的结构和发光性能进行了表征。XRD 和 EDS 结果证明了目标产物, 其由晶态的 LaPO_4 、 CePO_4 和非晶态的 SiO_2 构成; TEM 图显示样品形貌为不规则形状, 并且显示 $\text{CePO}_4\text{-6LaPO}_4\text{@4SiO}_2\text{:Eu}^{3+}$ 荧光粉形成核壳结构; HRTEM 图可以清楚地看出晶格条纹的形成; IR 谱图显示结果与 XRD 和 EDS 的分析结果一致; 荧光光谱图显示: 在 466 nm 激发下, $\text{CePO}_4\text{-6LaPO}_4\text{@4SiO}_2\text{:Eu}^{3+}$ 荧光粉在 615 nm 处出现属于 Eu^{3+} 的 $^5D_0 \rightarrow ^7F_2$ 跃迁的强烈红光发射。

关键词: 磷酸盐; 二氧化硅; 稀土离子; 荧光性能

中图分类号: O614.33¹; O614.33²; O614.33⁸

文献标识码: A

文章编号: 1001-4861(2019)09-1659-06

DOI: 10.11862/CJIC.2019.202

Luminescent Properties of a Red Phosphor $\text{CePO}_4\text{-6LaPO}_4\text{@4SiO}_2\text{:Eu}^{3+}$

LIU Ru WANG Xi-Gui*

(College of Chemistry and Environmental Science, Inner Mongolia Normal University, Hohhot 010022, China)

Abstract: $\text{CePO}_4\text{-6LaPO}_4\text{@xSiO}_2\text{:Eu}^{3+}$ phosphors were synthesized by sol-gel method and high temperature solid state method. The structure and luminescence property of the phosphors were characterized by X-ray diffraction (XRD), transmission electron microscope (TEM), energy dispersive spectra (EDS), infrared spectra (IR), excitation spectra and emission spectra. The results of XRD and EDS confirmed target product, which was made up of crystalline state LaPO_4 , CePO_4 and amorphous state SiO_2 ; TEM showed that the morphology of the sample was irregular and $\text{CePO}_4\text{-6LaPO}_4\text{@4SiO}_2\text{:Eu}^{3+}$ phosphor formed core-shell structure; HRTEM image clearly showed the formation of lattice fringes; IR study was consistent with the XRD and EDS study. The fluorescence spectra showed that under excitation with 466 nm, the $\text{CePO}_4\text{-6LaPO}_4\text{@xSiO}_2\text{:Eu}^{3+}$ phosphor gave a strongest red emission at the 615 nm that belongs to the $^5D_0 \rightarrow ^7F_2$ transition of Eu^{3+} .

Keywords: phosphate; silicon dioxide; rare earth ion; luminescence property

0 Introduction

In recent years, much attention has been paid to rare earth doped various phosphors, because it has the advantages of long-term stability, long lifetime and higher luminescent efficiency, etc. And it has been studied extensively for their potential applications in

light emitting devices, displays, solid state lasers, optical amplifiers, sensors and optoelectronics devices, etc.^[1-2]. Managing the red, green and blue light to get warm white light that makes our eyes feel comfortable. The use of red phosphor has more or less defects in recent years, which directly affects the quality of white luminescence. Therefore, the investigation of red

收稿日期: 2019-01-18。收修稿日期: 2019-07-05。

国家自然科学基金(No.21261010)、内蒙古自治区自然科学基金(No.2015MS0227)、内蒙古自治区创新基金项目(No.S20171013506)和内蒙古师范大学创新基金项目(No.CXJJS17081)资助项目。

*通信联系人。E-mail: wangxg@imnu.edu.cn

phosphor has an important theoretical significance and practical application value^[3-5].

In general, phosphors are composed of luminescent center and matrix materials. The rare earth Eu^{3+} shows red light under excitation with UV light and visible light and is an ideal red luminescence center. It is well known that due to the $f-f$ forbidden transition of rare earth ions. The absorption efficiency is low, so it is necessary to find some methods to enhance the absorption efficiency. The method commonly used to enhance the absorption efficiency is to dope rare earth ions as an activator to select a suitable matrix. The energy absorbs from the matrix effectively transmits to the activation center (rare earth ion) to improve the luminescent efficiency. This shows that the choice of matrix is crucial. Phosphates have the advantages of charge stabilization, excellent thermal stability, high chemical stability and other excellent properties. So the phosphates have become an important matrix material. Meanwhile, the silicon dioxide have the advantages of good chemical

stability, mechanical properties and low expansion coefficient. So it also becomes an excellent matrix material. But the reports about CePO_4 , LaPO_4 or SiO_2 as single matrix are very common^[3,6-10], the reports about CePO_4 , LaPO_4 and SiO_2 as composite matrix are unusual. In the paper, a novel red phosphor $\text{CePO}_4\text{-6LaPO}_4\text{:4SiO}_2\text{:Eu}^{3+}$ was successfully synthesized by sol gel method and high temperature solid state method. The structure and luminescence properties of $\text{CePO}_4\text{-6LaPO}_4\text{:4SiO}_2\text{:Eu}^{3+}$ phosphors also were investigated.

1 Experimental

1.1 Synthesis of samples

Firstly, the raw solution listed in Table 1 were added to clean beaker, which were stirred for 3 min. Then $\text{NH}_3\cdot\text{H}_2\text{O}$ was added to adjust pH value to 9 and kept stirring about 2 h to get a homogeneous sol. Secondly, the sol was transferred to a dry culture dish. After 2 days, it became a gel at room temperature. Next the samples were annealed at 900 °C for 17 hours. Finally, the samples were obtained.

Table 1 Experiment proportion of $\text{CePO}_4\text{-6LaPO}_4\text{:xSiO}_2\text{:Eu}^{3+}$

Solution	$V_{\text{TEOS}} / \text{mL}$	$V_{\text{EtOH}} / \text{mL}$	$V_{\text{La}(\text{NO}_3)_3 \cdot 6\text{H}_2\text{O}} / \text{mL}$	$V_{\text{Ce}(\text{NO}_3)_3 \cdot 6\text{H}_2\text{O}} / \text{mL}$	$V_{\text{EuCl}_3} / \text{mL}$	$V_{\text{H}_3\text{PO}_4} / \text{mL}$
1	0.76	4.24	9.00	1.50	4.39	10.50
2	1.13	3.87	9.00	1.50	4.39	10.50
3	1.50	3.50	9.00	1.50	4.39	10.50
4	1.89	3.11	9.00	1.50	4.39	10.50

1.2 Chemicals

$\text{NH}_3\cdot\text{H}_2\text{O}$ purchased from Tianjin Guangfu Fine Chemical Research Institute (98.0%), which was dissolved in distilled water to obtain $\text{La}(\text{NO}_3)_3$ solution. Eu_2O_3 was purchased from Baotou Rare Earth Institute (99.99%), which was dissolved in HCl solution to obtain EuCl_3 ($0.16 \text{ mol}\cdot\text{L}^{-1}$). H_3PO_4 was purchased from Tianjin Chemical Reagent Third Factory (85.0%). $\text{NH}_3\cdot\text{H}_2\text{O}$ was purchased from Tianjin Sailboat Chemical Reagent Technology Co., Ltd. (25%~28%). CH_3COOH was purchased from Tianjin Beilian Fine Chemicals Development Co., Ltd (99.7%).

1.3 Characterization

The X-ray diffraction (XRD) pattern of powder samples were measured on a Rigaku-Dmax 2500 X

diffractometer equipped with Cu $K\alpha$ radiation ($\lambda = 0.154\,05 \text{ nm}$, $U=40 \text{ kV}$, $I=30 \text{ mA}$, $2\theta=10^\circ\sim 80^\circ$); A 200 keV JEOL 2010 (HRTEM) micro-scope was used to record Transmission Electron Microscopy (TEM) images; IR spectra was acquired with using a Hitachi U-4100 UV-VIS-NIR spectrometer with the KBr pellet technique; The excitation and emission spectra were measured with using a F-4500 spectrophotometer equipped with a 150 W xenon lamp as the excitation source.

2 Results and discussion

2.1 XRD study

XRD patterns of $\text{CePO}_4\text{-6LaPO}_4\text{:Eu}^{3+}$ and $\text{CePO}_4\text{-6LaPO}_4\text{:4SiO}_2\text{:Eu}^{3+}$ phosphors were reported in Fig.1.

For SiO_2 particles, no diffraction peak was observed, excepted for a very small broad peak at $2\theta = 22^\circ$, characteristic of amorphous silica^[11-12]. In addition, all the diffraction peaks of $\text{CePO}_4\text{-6LaPO}_4\text{:Eu}^{3+}$ phosphor were agreed with the standard card (PDF No.32-0199 and No.46-1326). The indicated that a low amount of SiO_2 almost did not affect the crystal structure of phosphate. The above results showed that the sample was made up of crystalline state CePO_4 , LaPO_4 and amorphous state SiO_2 . Note that the intensity diffraction peaks of $\text{CePO}_4\text{-6LaPO}_4\text{:Eu}^{3+}$ phosphor were a little improved than those of $\text{CePO}_4\text{-6LaPO}_4\text{:Eu}^{3+}$ phosphor, suggesting that the size of the crystalline grains of phosphate on the surfaces of the silica particles in the composite was smaller than that in the pure phosphate. At the same time, no impurity peak from the third phase was detected, which indicated Eu^{3+} entered lattice in the matrix and occupied the site of La^{3+} and Ce^{3+} in the matrix to form a stable solid solution without affecting the

structure of host lattice.

According to previous reports^[10,12], to form a new solid solution, the radius in the percentage difference (D_r) between the doped ions and the possibly substituted ion should be less than 15%, see the following formula:

$$D_r = \frac{R_1(\text{CN}) - R_2(\text{CN})}{R_1(\text{CN})} \times 100$$

Where $R_1(\text{CN})$ is the radius of the matrix cation and $R_2(\text{CN})$ is the radius of the doped ions. Herein, the values of $R_1(\text{CN})$ (Ce^{3+} and La^{3+}) and $R_2(\text{CN})$ (Eu^{3+}) are respectively 0.103, 0.106 and 0.095. According to this formula, the D_r value respectively was 7.8% and 10.4%, and less than 15%, further confirmed that the Eu^{3+} occupied the site of the La^{3+} and Ce^{3+} in the matrix to form a stable solid solution without affecting the structure of the CePO_4 and LaPO_4 host lattice.

2.2 TEM study

TEM image of $\text{CePO}_4\text{-6LaPO}_4\text{:Eu}^{3+}$ phosphor was reported in Fig.2(a). It showed that the grain morphology was irregular shape. The grain size was measured by Nano Measure App and was 0.38 μm . According to the XRD data, the grain size was calculated by Scherrer Formula and was 0.31 μm . Both results were consistent.

Fig.2 (b) showed TEM image of $\text{CePO}_4\text{-6LaPO}_4\text{:Eu}^{3+}$ phosphor, $\text{CePO}_4\text{-6LaPO}_4\text{:Eu}^{3+}$ phosphor was further sub-jected to TEM analysis to determine the core-shell structure. The core-shell structure of the sample could be seen clearly due to the different electron penetrability of the core and shell. The core could be seen as a black irregular sphere and the shells had a gray color.

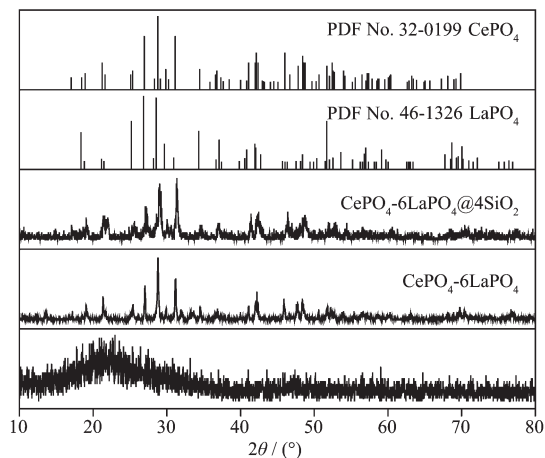


Fig.1 XRD patterns of $\text{CePO}_4\text{-6LaPO}_4\text{:Eu}^{3+}$ and $\text{CePO}_4\text{-6LaPO}_4\text{:Eu}^{3+}$

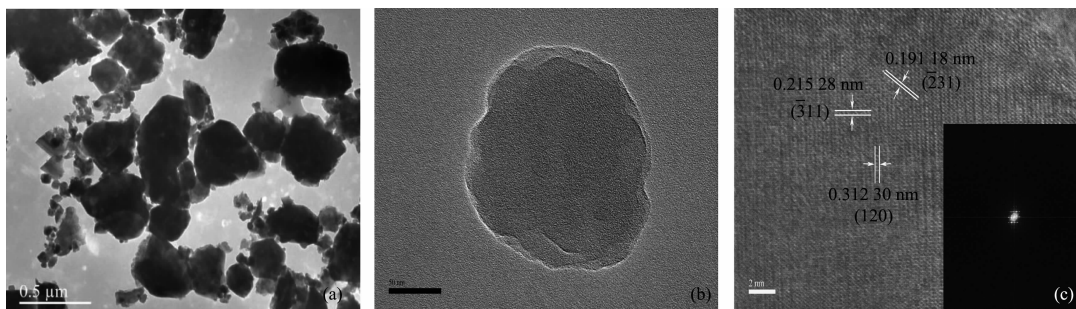


Fig.2 TEM images (a, b) and HRTEM image (c) of $\text{CePO}_4\text{-6LaPO}_4\text{:Eu}^{3+}$ phosphor

The HRTEM image of $\text{CePO}_4\text{-6LaPO}_4\text{:4SiO}_2\text{:Eu}^{3+}$ phosphor was reported in Fig.2(c). It clearly showed the $\text{CePO}_4\text{-6LaPO}_4\text{:4SiO}_2$ lattice and lattice fringes with an inter-planar spacing of 0.191 18, 0.215 28 and 0.312 30 nm, which had good match with those of the standard pattern of PDF card ($\text{LaPO}_4/\text{CePO}_4$), i.e., spacing for ($\bar{2}31$) 0.191 18 nm, ($\bar{3}11$) 0.215 28 nm and (120) 0.312 30 nm.

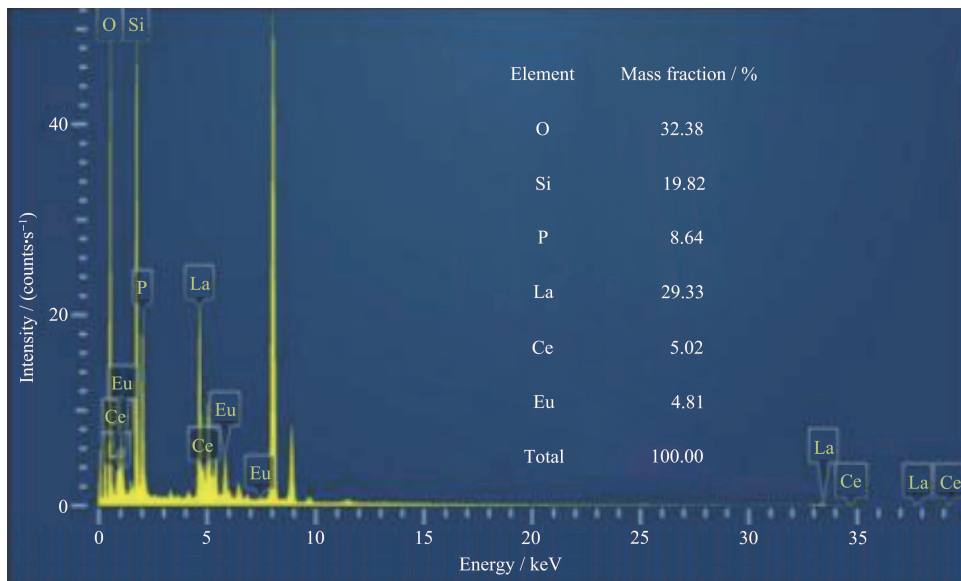


Fig.3 EDS energy spectrum of the $\text{CePO}_4\text{-6LaPO}_4\text{:4SiO}_2\text{:Eu}^{3+}$ phosphor

2.4 IR study

IR spectra of $\text{CePO}_4\text{-6LaPO}_4\text{:Eu}^{3+}$ and $\text{CePO}_4\text{-6LaPO}_4\text{:4SiO}_2\text{:Eu}^{3+}$ phosphor were reported in Fig.4. The absorption bands from 1 600 cm^{-1} to 400 cm^{-1} were observed, which had different infrared absorption peaks. In the spectra of $\text{CePO}_4\text{-6LaPO}_4$ as the matrix, the three peaks at 1 089, 1 063 and 1 016 cm^{-1} were obtained by cleaving at 992 cm^{-1} and corresponded the asymmetric stretching vibration peak of P-O, which was the characteristic of monoclinic phosphates^[17]. In the spectra of $\text{CePO}_4\text{-6LaPO}_4\text{:4SiO}_2$ as the matrix, the absorption peaks at 1 107 cm^{-1} belonged to anti-stretching vibration peak of Si-O-Si. The absorption peaks located at 992, 952 cm^{-1} were observed in the region of the stretching vibration of PO_4^{3-} group. The absorption peak at 797 cm^{-1} was stretching vibration peak of Si-O-Si. The band located at 621 cm^{-1} was observed in the region of O=P-O bending vibrations (it compared with the $\text{CePO}_4\text{-6LaPO}_4$ as the matrix, the

2.3 EDS study

The EDS spectrum of $\text{CePO}_4\text{-6LaPO}_4\text{:4SiO}_2\text{:Eu}^{3+}$ phosphor was reported in Fig.3. The elements of O, Si, P, La, Ce and Eu were observed in the spectrum, and the ratio of La, Ce and Si elements was 6:1:4, which clearly indicated the formation of $\text{CePO}_4\text{-6LaPO}_4\text{:4SiO}_2\text{:Eu}^{3+}$ phosphor.

peak position occurred blue shift). The bands at 575, 559 and 537 cm^{-1} were the bending vibrations of O-P-O^[13-14] (it compared with $\text{CePO}_4\text{-6LaPO}_4$ as the matrix, the peak at 537 cm^{-1} occurred red shift). The absorption peak at 466 cm^{-1} was bending vibration peak of Si-O-Si (it compared with $\text{CePO}_4\text{-6LaPO}_4$ as matrix, the peak position occurred red shift). According to the above

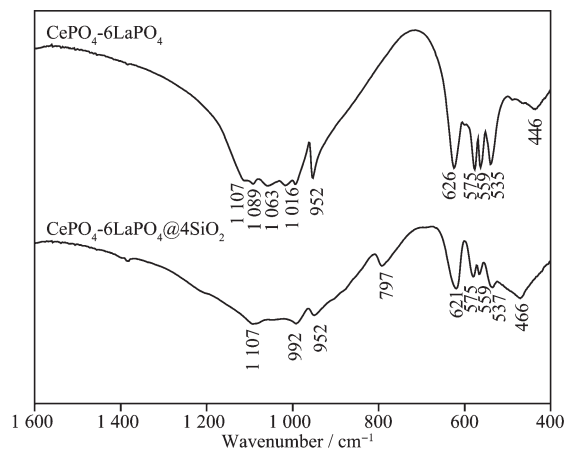


Fig.4 IR spectra of $\text{CePO}_4\text{-6LaPO}_4\text{:4SiO}_2\text{:Eu}^{3+}$ phosphor

analysis, it showed that the sample was made up of phosphate and silicon dioxide, which was consistent with the result of XRD study.

The polarization of Eu^{3+} was bigger than $\text{La}^{3+}/\text{Ce}^{3+}$, Eu^{3+} replaced $\text{La}^{3+}/\text{Ce}^{3+}$, which caused a slight change in the shape of PO_4^{3-} electron cloud. So the infrared vibration peak of PO_4^{3-} caused red shift and blue shift in different degrees.

2.5 Luminescence study

2.5.1 Excitation and emission spectrum of $\text{CePO}_4\text{-6LaPO}_4\text{@}x\text{SiO}_2\text{:Eu}^{3+}$

The excitation spectra of core-shell structure $\text{CePO}_4\text{-6LaPO}_4\text{@}x\text{SiO}_2\text{:Eu}^{3+}$ were reported in Fig.5. The excitation spectrum consisted of two sharp peaks at 395 and 466 nm, and the peaks corresponded to the transitions from 7F_0 to 5L_6 (395 nm) and 5D_2 (466 nm). The emission intensity was strongest at 466 nm, so 466 nm was selected as the optimum excitation wavelength.

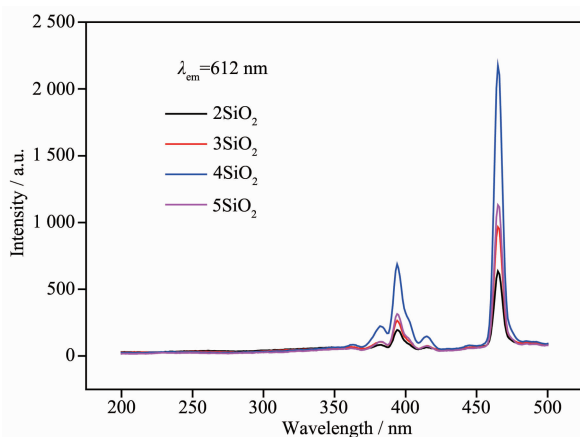


Fig.5 Excitation spectra of $\text{CePO}_4\text{-6LaPO}_4\text{@}x\text{SiO}_2\text{:Eu}^{3+}$

The emission spectra of core-shell structure $\text{CePO}_4\text{-6LaPO}_4\text{@}x\text{SiO}_2\text{:Eu}^{3+}$ phosphor were reported in Fig.6. The emission peaks of 588 and 615 nm corresponded to the transitions from 5D_0 to 7F_1 and 7F_2 , respectively. The core shell $\text{CePO}_4\text{-6LaPO}_4\text{@}x\text{SiO}_2\text{:Eu}^{3+}$ had a luminous intensity that increased first and then decreased with the increased of SiO_2 in the matrix, and there is an optimal core-shell ratio. The shell thickness was measured by the molar ratio of core to the element contained in the shell^[18], when the core shell ratio was 1:4, the sample had the brightest red light at 615 nm. Because a large amount of Eu^{3+} was surrounded by SiO_2 and even diffuses into the SiO_2

network structure, greatly reducing the possibility of Eu^{3+} being in the surface state. That is to say, the appearance of the core-shell structure increased the distance between Eu^{3+} and the surface, thus changing the surrounding matrix environment of Eu^{3+} near the original surface (from unevenness to relatively uniform), which hindered the energy transfer of the original Eu^{3+} and surface states, so that improved luminous intensity of the sample. When the core shell ratio was more than 1:4, the luminescence intensity gradually decreased. As the thickness of the shell continued to increase, the thicker shell provided a uniform matrix environment. But the loss of light through the more, which led to the excitation light could be finally utilized became less, so that causing the emitted light to weaken. The above results indicated that the optimum ratio of phosphate to SiO_2 was 1:4.

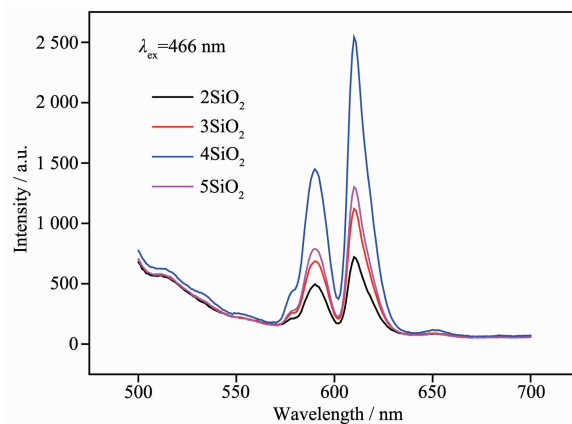


Fig.6 Emission spectra of $\text{CePO}_4\text{-6LaPO}_4\text{@}x\text{SiO}_2\text{:Eu}^{3+}$

2.5.2 Luminescence study of $\text{CePO}_4\text{-6LaPO}_4\text{@}4\text{SiO}_2\text{:Eu}^{3+}$ and $\text{CePO}_4\text{-6LaPO}_4\text{:Eu}^{3+}$ phosphors

The emission spectra of $\text{CePO}_4\text{-6LaPO}_4\text{@}4\text{SiO}_2\text{:Eu}^{3+}$ were reported in Fig.7. Before the addition of SiO_2 , the main peak of $\text{CePO}_4\text{-6LaPO}_4\text{:Eu}^{3+}$ phosphor was located at 588 nm. After the addition of SiO_2 , the main peak of $\text{CePO}_4\text{-6LaPO}_4\text{@}4\text{SiO}_2\text{:Eu}^{3+}$ phosphor was located at 615 nm. The showed that the addition of SiO_2 effectively increased red light intensity of the sample.

The sample emitted orange light and red light, which was closely related to the crystallographic position of Eu^{3+} ^[15-16]. The transition $^5D_0 \rightarrow ^7F_1$ was dominant when Eu^{3+} occupied the lattice site with inversion center, and the sample emitted orange light

(the main peak was located at 588 nm). The transition $^5D_0 \rightarrow ^7F_2$ was dominant when Eu^{3+} occupied the lattice site without inversion center, and the sample emitted red light (the main peak was located at 615 nm). In the experiment, the Eu^{3+} of $\text{CePO}_4\text{-6LaPO}_4\text{:Eu}^{3+}$ phosphor occupied the lattice site with inversion center, so the sample emitted orange light; the Eu^{3+} of $\text{CePO}_4\text{-6LaPO}_4\text{:Eu}^{3+}$ phosphor occupied the lattice site without inversion center, so the sample emitted red light. It as shown as Fig.8. The intensity pattern of the emission lines demonstrate that the Eu^{3+} was successfully doped in the sample. In addition, the formation of core-shell structure was also beneficial to red luminescence^[18-19].

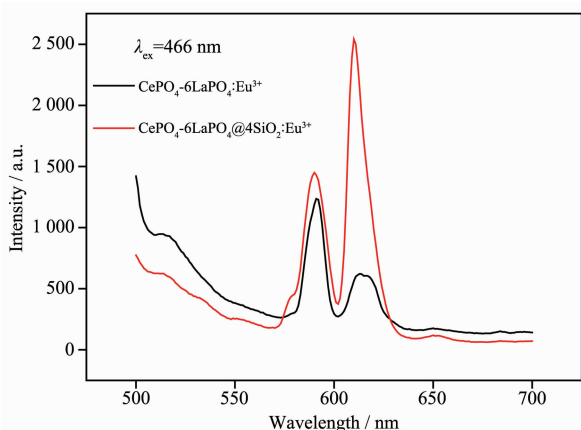


Fig.7 Emission spectra of $\text{CePO}_4\text{-6LaPO}_4\text{:Eu}^{3+}$ and $\text{CePO}_4\text{-6LaPO}_4\text{:Eu}^{3+}$

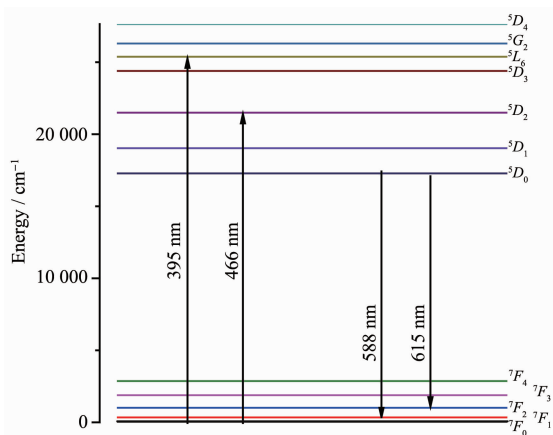


Fig.8 Energy level diagram

3 Conclusions

The $\text{CePO}_4\text{-6LaPO}_4\text{:Eu}^{3+}$ red phosphors were synthesized by sol gel method and high temperature solid statue method. The results showed that the optimal excitation wavelength of the phosphor was 466

nm and the optimum ratio of phosphate to SiO_2 was 1:4. And the appearance of core-shell structure $\text{CePO}_4\text{-6LaPO}_4\text{:Eu}^{3+}$ was more conducive to the doping of Eu^{3+} and improved the red light of the sample. It indicated that $\text{CePO}_4\text{-6LaPO}_4\text{:Eu}^{3+}$ could be a good candidate as red phosphor or it combined with blue and green phosphor to get ideal quality warm WLED.

References:

- [1] Du P, Yu J S. *J. Lumin.*, **2016**,**179**:451-456
- [2] Li K, Lian H Z, Shang M M, et al. *Dalton Trans.*, **2015**,**44** (47):20542-20550
- [3] Yang J Y, Jia X H, Zeng X D, et al. *J. Mater. Sci.*, **2015**,**50** (12):4405-4411
- [4] JIN Ye(金叶), QIN Wei-Ping(秦伟平), ZHANG Ji-Sen(张继森), et al. *Spectrosc. Spect. Anal.* (光谱学与光谱分析), **2008**,**28**(12):2768
- [5] Gupta S K, Ghosh P S, Sahu M, et al. *RSC Adv.*, **2015**,**5** (72):58832-58842
- [6] WANG Xi-Gui(王喜贵), WU Hong-Ying(吴红英), XIE Da-Tao(谢大弢), et al. *J. Rare Earth*(中国稀土学报), **2002**,**20** (3):172-176
- [7] WU Xue-Yan(吴雪艳), YOU Hong-Peng(尤洪鹏), ZENG Xiao-Qing(曾小青), et al. *Chem. J. Chinese Universities*(高等学校化学学报), **2003**,**24**(1):1-4
- [8] Hatada N, Nose Y, Kuramitsu A, et al. *J. Mater. Chem.*, **2011**,**21**(24):8781-8786
- [9] Cao M H, Hu C W, Wu Q Y, et al. *Nanotechnology*, **2005**, **16**(2):282-286
- [10] Riwotzki K, Meyssamy H, Kornowski A, et al. *J. Phys. Chem. B*, **2000**,**104**(13):2824-2828
- [11] Zhang J M, Zhao D L, Zhang D D, et al. *Asian J. Chem.*, **2014**,**26**:2211-2214
- [12] Musi S, Filipovi-Vincekovi N, Sekovani L, et al. *J. Chem. Eng.*, **2011**,**28**:89-94
- [13] Ray S, Nair G B, Tadge P, et al. *J. Lumin.*, **2018**,**194**:64-71
- [14] Krishna B L, Jeon Y I, Yu J S. *J. Alloy Compd.*, **2014**,**614**: 443-447
- [15] WANG Xi-Gui(王喜贵), BO Su-Ling(薄素玲), QI Xia(齐霞), et al. *Chinese J. Inorg. Chem.*(无机化学学报), **2009**,**25**(2): 350-353
- [16] CAO Jiao-Lan(曹娇兰), WANG Xi-Gui(王喜贵). *Chinese J. Inorg. Chem.*(无机化学学报), **2018**,**34**(2):325-330
- [17] Zhao M L, Li G S, Li L P. *Cryst. Growth Des.*, **2012**,**12**: 3983-3991
- [18] Lim M A, Seok II S, Ghung W J, et al. *Opt. Mater.*, **2008**, **31**(2):201-205
- [19] LIU Gui-Xia(刘桂霞), LI Ruo-Lan(李若兰), DONG Xiang-Ting(董向婷), et al. *Chin. J. Lumin.*(发光学报), **2011**,**32**(5): 466-470